Molecular Interactions in 1-Ethyl-3-methylimidazolium Acetate Ion Pair: A Density Functional Study

Nilesh R. Dhumal,[†] Hyung J. Kim,*[,†,‡] and Johannes Kiefer[§]

Department of Chemistry, Carnegie Mellon University, Pittsburgh, Pennsylvania 15213, School of Computational Sciences, Korea Institute for Advanced Study, Seoul 130-722, Korea, and Lehrstuhl fuer Technische Thermodynamik and Erlangen Graduate School in Advanced Optical Technologies, University Erlangen-Nuremberg, D-91058 Erlangen, Germany

Received: July 31, 2009

The density functional method is used to obtain the molecular structure, electron density topography, and vibrational frequencies of the ion pair 1-ethyl-3-methylimidazolium acetate. Different conformers are simulated on the basis of molecular interactions between the 1-ethyl-3-methylimidazolium cation and acetate anion. The lowest energy conformers exhibit strong C−H···O interionic interactions compared with other conformers. Characteristic vibrational frequencies of the ion pair and their shifts with respect to free ions are analyzed via the natural bond orbitals and difference electron density maps coupled with molecular electron density topology. Theoretically scaled vibrational frequencies are also compared with the spontaneous Raman scattering and attenuated total reflection infrared absorption measurements.

1. Introduction

In recent years room-temperature ionic liquids (RTILs) consisting of bulky cations paired with a variety of different anions have gained wide popularity because of their unique properties and wide range of applications. RTILs are characterized by low melting points, negligible vapor pressure and nonflammability as well as good thermal and chemical stability, particularly in the presence of air and moisture.[1−6] As such, they provide an environmentally friendly alternative to toxic organic solvents for chemical synthesis, separations and extractions. Due to their high intrinsic conductivity and wide electrochemical window, RTILs are also an excellent candidate for electrolytes in many electrochemical devices.

Needless to say, interionic interactions, which will also be referred to as molecular interactions hereafter, play a central role in the determination of RTIL properties, such as transport and phase behaviors. Thus proper understanding of molecular interactions is crucial to, e.g., design and selection of RTILs for a variety of different applications. In this context, a theoretical analysis of RTIL electronic structure via the molecular orbital methods can provide very useful insights into the roles of molecular interactions. Also computer simulations offer a powerful tool to analyze RTIL properties in the solution phase.[7] Among available experimental methods, spectroscopic techniques play a particularly important role in understanding the characteristics of RTILs and the special nature of their interactions. For instance, vibrational spectroscopy, including infrared (IR) and Raman spectroscopy, has proven to be very useful in the analysis and classification of molecular structures. A recent summary of vibrational studies of RTILs containing 1-ethyl-3-methylimidazolium cations can be found in ref 8.

Perhaps the most promising and insightful approach to understanding molecular physics, such as origins of frequency shifts and/or intensity changes in vibrational spectra, of RTILs and other systems, is combining theoretical and experimental methods. In the present work, we employ this approach to study molecular interactions of the ion pair 1-ethyl-3-methylimidazolium acetate and their influence on its conformation. There have been significant efforts recently to understand vibrational spectra of related ionic liquid systems via quantum chemistry methods.[9] Here we make a detailed comparison between theoretical predictions and experimental measurements with account of different conformations of ions and ion pairs. The reason we choose 1-ethyl-3-methylimidazolium acetate is that it has many applications of practical importance. For example, its potential to dissolve carbohydrates makes 1-ethyl-3-methylimidazolium acetate a very good candidate as solvent media for biomass conversion and production of alternative fuels.[10] Also it is not toxic to bioactive substances such as enzymes, so that it can be used in bioprocess engineering, e.g., in the selective production of pharmaceuticals with enzymes immobilized in the RTIL phase.[11]

By employing the density functional theory (DFT) description, different conformers of 1-ethyl-3-methylimidazolium acetate ion pair are classified on the basis of their energies and molecular interactions between the constituent cation and anion. Manifestations of these interactions are discussed in detail. Theoretically scaled vibrational frequencies are also compared with the experimental Raman and IR spectra. The directions of frequency shifts with respect to isolated ions are analyzed via the difference electron density coupled with electron density topography.

The outline of this paper is as follows: A brief description of the computational and experimental methods employed in this work is given in sections 2 and 3, respectively. The geometry, normal mode vibrations and electron density topography of the ion pair 1-ethyl-3-methylimidazolium acetate are analyzed in section 4. A comparison with experimental results on vibrational frequencies is also made there. Section 5 concludes.

* Corresponding author. E-mail: hjkim@cmu.edu.
[†] Carnegie Mellon University.
[‡] Korea Institute for Advanced Study.
[§] University Erlangen-Nuremberg.

10.1021/jp907394v CCC: $40.75
Published on Web 08/27/2009

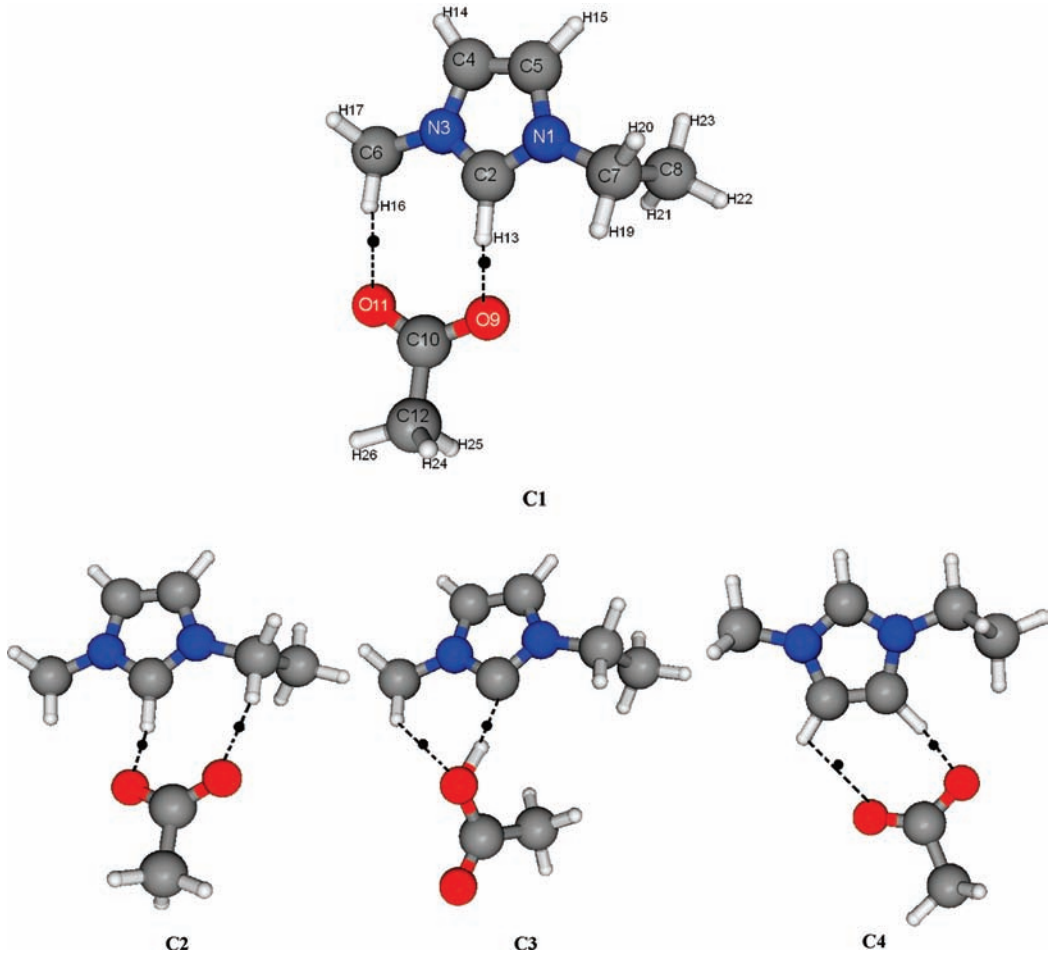

Figure 1. Optimized geometries of four lowest energy conformers of the 1-ethyl-3-methylimidazolium acetate ion pair. Filled circles in black show the bond critical points.

2. Computational Method

Geometry optimization calculations were performed on isolated 1-ethyl-3-methylimidazolium and acetate ions as well as their ion pair using the hybrid density functional theory, which incorporates Becke's three-parameter exchange with the Lee, Yang, and Parr correlation functional[12,13] method (B3LYP). We employed the GAUSSIAN-03 program[14] with the internally stored 6-31G(d,p) and 6-31++G(d,p) basis sets. For additional insight, we further optimized geometries of individual ions and ion pairs and calculated their energies using the second-order Møller−Plesset (MP2) perturabation theory with the 6-31G(d,p) basis set. The stationary point geometries were confirmed to be the local minima on the potential energy surface by analyzing the vibrational frequencies, which were found to have no imaginary components. Normal modes were assigned by visualizing the displacement of atoms around their equilibrium positions using the UNIVIS-2000 visualization package.[15] Natural bond orbital analysis was performed on the basis of DFT (B3LYP/6-31G(d,p)).[16] Molecular electron density topography was studied[14,17] and critical points were identified. These include: maxima (3, 3), e.g., nuclear positions, minima (3, −3) generally known as cage critical points and two types of saddle points, (3, −1) and (3, +1), respectively referred to as the bond critical and ring critical points. Here R and σ of (R, σ) represent, respectively, the number and algebraic sum of eigenvalues of the Hessian matrix. Difference electron density $\Delta\rho$ was calculated via $\Delta\rho = \rho_{\text{complex}} - (\rho_{\text{free anion}} + \rho_{\text{free cation}})$, where the subscripts free cation and anion denote that the individual ions comprising the ion pair complex are in vacuo. Finally, difference electron density maps were derived.

For later use, the atomic numbering scheme used in the present work is displayed in Figure 1a.

3. Experimental Method

Chemical. The ionic liquid 1-ethyl-3-methylimidazolium acetate was prepared from 1-ethyl-3-methylimidazolium hydroxide and acetic acid ("Essigsaeure 100% wasserfrei", purchased from Merck KGAA). Further details can be found in ref 18 and the references therein. After synthesis, water was removed using a rotary evaporator and the ionic liquid was dried at room temperature under vacuum for 24 h. The chemical identity and purity of the yielded 1-ethyl-3-methylimidazolium acetate was also confirmed by ^{1}H NMR measurement.

Infrared Spectroscopy. The IR spectrum from 550 to 4000 cm^{-1} was recorded with a Nicolet Model 360 FTIR at 2 cm^{-1} resolution. The device operates in attenuated total reflection (ATR) mode. For this purpose it is equipped with a diamond crystal at whose surface the evanescent electromagnetic field interacted with the sample. The number of reflections is 1 and the penetration depth of the system is approximately 1/5 of the wavelength. In the IR spectrum shown in section 4 below, the wavelength dependence of the penetration depth is taken into consideration.

Raman Spectroscopy. The experimental Raman setup consisted of a grating stabilized diode laser operating at 785 nm which was focused into a quartz glass cuvette filled with the

TABLE 1: Relative Stabilization (in kJ mol^{-1}) Energies of Different Conformers of 1-Ethyl-3-methylimidazolium Acetate Ion Pair[a]

conformers	MP2/6-31G**	B3LYP/6-31++G**	B3LYP/6-31G**
C1	2.95 (1.55)	0.00 (0.00)	0.00 (0.00)
C2	0.00 (0.00)	0.49 (0.49)	0.71 (0.54)
C3	28.43 (27.19)	32.87 (33.12)	25.16 (27.99)
C4	50.93 (48.99)	51.86 (52.11)	55.76 (46)

[a] Zero point corrected energies are displayed in parentheses.

ionic liquid. The scattered light was collected by an achromatic lens, filtered by a long-pass filter (790 nm cutoff wavelength) and dispersed in a spectrograph with an integrated charge-coupled-device chip for signal detection. The spectral resolution of the system was approximately 2−3 cm^{-1} varying with wavelength. The described system allows recording Raman spectra in the range 200−2000 cm^{-1}.

4. Results and Discussion

Four different conformers **C1**−**C4** we found for the ion pair 1-ethyl-3-methylimidazolium acetate are displayed in Figure 1. The dashed lines there denote the molecular interactions between the anion and cation. For simplicity, the distance between two moieties of the ions was employed as the main criteria for the existence of the molecular interactions. Specifically, if the separation between the H atom of a C−H bond of the cation and an O atom of the anion is less than 2.5 Å, we treat their C−H···O as a molecular interaction.[19] We nonetheless point out that all interionic interactions thus identified have a bond critical point, i.e., critical point of type (3, −1) mentioned above, which is marked as a filled circle in Figure 1. The **C1**, **C2**, and **C4** conformers all exhibit two C−H···O molecular interactions. We notice that **C1** and **C2** show very similar interaction structures. The only difference between the two is whether it is H of C6 or of C7 in addition to H of C2 that interacts with O atoms of the anion. It is also interesting that in **C3**, proton transfer occurs from C2 of the cation to O9 of the anion, while other conformers do not show proton transfer. Thus the **C3** conformer is characterized by one C−H···O and one C···H−O interionic interaction.

Relative energies of the four different conformers obtained with different methods are compared in Table 1. The **C3** and **C4** conformers are considerably higher in energy than **C1** and **C2**. As expected from the interaction structures in Figure 1, **C1** and **C2** are very close in energy. In fact, their difference in the zero-point corrected energy is less than the thermal energy at room temperature. Thus we will consider mainly these two lowest energy conformers below, especially in the analysis of vibrations.

Conformer Geometry. The results for geometrical parameters for different conformers obtained with the B3LYP/6-31G** method are compiled in Table 2. For comparison, the bond lengths for free states of the cation and anion, i.e., isolated ions, are also presented there. Other methods we studied yield essentially the same results and thus are not considered here. We notice that, generally, C−H bonds that participate in the interionic interactions, i.e., dashed lines in Figure 1, become extended in all four conformers, compared to the corresponding bonds of a free cation. For example, the C2−H13 bond of **C1** and **C3** show a significant elongation; compared to the free cation value 1.079 Å, its bond length increases by 0.094 and 0.092 Å, respectively. With the exception of C2−H13 of **C3** that becomes deprotonated, the elongation of the C2−H13 bond of the **C1** conformer is the largest among all C−H bonds in the four conformers of Figure 1. If we can assume that the elongation and thus weakening of a bond participating in interionic interactions are a good indicator of the interaction strength, our analysis predicts that the C2−H13···O9 interaction of **C1** is the strongest among all C−H···O type interactions identified in the four conformers. This captures well the highly acidic character of hydrogen atoms at the H13 position of imidazolium compounds, which allows strong intermolecular interactions involving these H atoms.[20] The C−O bonds of the anion, which also participate in the interionic interactions in all four conformers, show a behavior similar to C−H bonds.

TABLE 2: Calculated Bond Distances (in Å) in Cation, Anion and Different Conformers of 1-Ethyl-3-methylimidazolium Acetate Ion Pair

	anion	cation	C1	C2	C3	C4
N1−C2		1.338	1.344	1.341	1.362	1.340
C2−N3		1.339	1.341	1.344	1.363	1.343
N3−C4		1.383	1.386	1.386	1.389	1.387
C4−C5		1.364	1.362	1.362	1.357	1.364
N3−C6		1.470	1.469	1.463	1.460	1.460
N1−C7		1.483	1.472	1.478	1.463	1.474
C7−C8		1.526	1.527	1.526	1.529	1.528
O9−C10	1.257		1.282	1.282	1.340	1.280
C10−O11	1.257		1.251	1.251	1.213	1.254
C10−C12	1.575		1.532	1.532	1.524	1.538
C2−H13		1.079	1.173	1.171	1.783[a]	1.078
C4−H14		1.079	1.078	1.078	1.079	1.079
C5−H15		1.078	1.078	1.078	1.079	1.133
C6−H16		1.089	1.100	1.091	1.090	1.091
C6−H17		1.091	1.093	1.093	1.094	1.092
C6−H18		1.091	1.093	1.093	1.094	1.092
C7−H19		1.092	1.092	1.099	1.092	1.094
C7−H20		1.093	1.094	1.094	1.095	1.094
C8−H21		1.093	1.094	1.094	1.094	1.094
C8−H22		1.093	1.093	1.094	1.094	1.094
C8−H23		1.093	1.095	1.096	1.095	1.095
C12−H24	1.097		1.095	1.091	1.090	1.092
C12−H25	1.097		1.095	1.095	1.094	1.095
C12−H26	1.100		1.094	1.095	1.096	1.096
O9----H13			1.510	1.514	1.020[a]	
O11----H16			2.008			
O11----H19				2.030		
O9----H5						1.630
O11----H4						2.412

[a] In the **C3** conformer the H13 proton transfers to anion.

In contrast, nonparticipating bonds generally become shortened upon the formation of an ion pair. A good example is the C10−C12 bond of the acetate ion, which exhibits a significant reduction in its bond length in all four conformers, compared to the free anion value. For the imidazolium ion, bond contraction occurs for the N1−C7, N3−C6, and C4−C5 bonds. These results expose that the molecular interactions between constituent ions of the ion pair exert a significant influence on and thus introduce substantial changes in their geometry.

Vibration. Geometrical changes induced by the formation of a composite system, such as the ion pair considered here, are often accompanied by shifts in vibrational frequencies with respect to those of its constituents. Therefore, spectroscopic analysis of the normal vibrational modes and their frequency shifts provide a useful tool to probe molecular interactions among the constituents of the composite system and offer an excellent testing ground for theoretical methods. Indeed, it is well established that, in general, normal vibrations derived from the DFT (B3LYP) method yield a better agreement with measurements than those determined with the Møller−Plesset

TABLE 3: Selected Vibrational Frequencies (in cm^{-1}) of Free Cation, Anion and C1 and C2 Conformers of 1-Ethyl-3-methylimidazolium Acetate Ion Pair[a]

	theoretical scaled vibrations				experimental	
vibration	cation	anion	C1	C2	infrared	Raman
C4−H14, C5−H15 asym stretch	3198 (16)					
C8−H22 stretch					3148	
C6−H17 stretch	3093 (0)		3054 (10)	3048 (12)	3091	
asymm. H19−C7−H20 stretch	3062 (9)		3030 (18)	3045 (20)	2983	
			2982 (22)	3004 (43)		
asymm. H16−C6−H18 stretch			3017 (55)	3029 (10)		
C7−H19 stretch				3004 (43)		
				2915 (265)		
C6−H16 stretch			2896 (285)		2879	
symm. H17−C6−H18 stretch	3002 (6)		3046 (16)	2973 (34)		
				2958 (13)		
H24−C12−H25 asym stretch		2993 (90)	3056 (29)	3056 (29)		
H25−C12−H26 asym stretch		2968 (81)	3018 (29)	3018 (25)		
H24−C12−H26 asym stretch		2907 (45)	2964 (15)	2956 (14)		
C2−H13 stretch	3202 (30)		2005 (1973)	2024 (1974)		
O9−C10 stretch		1702 (423)			1701	1699
N3−C4−H14 rock + O9−C10 stretch			1642 (242)		1647	
N1−C2−H13 rock	1570 (32)		1573 (47)	1569 (35)	1566	1569
N3−C4−H14 rock	1562 (54)		1543 (171)	1547 (182)		
H19−C7−H20 scissor	1473 (15)					
H16−C6−H17 scissor	1456 (9)		1491 (13)	1491 (12)		
H22−C8−H23 scissor	1460 (16)		1481 (23)	1480 (11)	1466	
H16−C6−H18 rock	1448 (16)		1443 (19)	1464 (11)	1449	1454
H24−C12−H25 scissor		1450 (0)	1438 (29)	1438 (27)	1424	1421
H21−C8−H22 rock	1395 (7)		1392 (182)	1398 (119)	1388	1393
H19−C7−H20 rock	1349 (14)		1415 (14)			
C10−C12 stretch		1333 (266)	1387 (169)	1381 (217)		
H19−C7−H20 rock			1368 (32)	1360 (92)	1362	
H19−C7−H20 rock			1349 (26)			
H24−C12−H25 rock		1280 (15)	1331 (26)	1331 (47)	1332	1336
N1−C7 stretch	1311 (11)		1319 (49)	1321 (53)		
H19−C7−H20 twist	1278 (0)		1304 (308)	1315 (159)		
H19−C7−H20 twist	1237 (0)		1256 (117)	1247 (190)	1253	1254
N1−C2−H13 twist	1148 (108)		1186 (63)	1186 (59)	1170	1174
			1129 (11)	1145 (15)	1120	1114
				1109 (34)		
H16−C6−H17 wag	1119 (0)		1090 (36)	1084 (13)	1089	1090
CCH scissor	1096 (9)		1060 (54)	1073 (16)	1046	1023
				1062 (43)		
H24−C12−H26 wag			991 (10)		1005	
Symm. C2−N3−C4 stretch	1008 (0)		956 (163)	960 (171)	958	958
O9−C10−O11 bend		837 (72)	882 (173)	882 (157)	876, 845	886
N1−C2−H13 wag	805 (38)			804 (12)	802	802
C4−C5−H15 wag	729 (21)		713 (36)	713 (35)	757, 701	701
			628 (89)			
CN bond oscillation	642 (15)		647 (13)	651 (13)	648, 621	647
			618 (11)	628 (90)		

[a] The vibrational intensity (units: km/mol) is reported in parentheses.

perturabation method.[21] As for DFT, our calculations indicate that the predictions of B3LYP/6-31G(d,p) tend to agree better with experiments in both vibrational frequencies and multiplet structures than those of B3LYP/6-31++G(d,p). A similar observation was made also in ref 22. Therefore, we will consider only the results of B3LYP/6-31G(d,p) hereafter. For the B3LYP/6-31++G(d,p) (and MP2/6-31(d,p)) results on vibrations and their comparison with B3LYP/6-31G(d,p), the reader is referred to the Supporting Information.

In Table 3, we compare vibrational frequencies of the 1-ethyl-3-methylimidazolium cation, acetate anion, and **C1** and **C2** conformers of their ion pair derived from the B3LYP density functional theory in the frequency region 600−3200 cm^{-1}. The harmonic frequencies presented there are the DFT results scaled by a factor 0.97 as in many prior studies.[21,22] For comparison, experimental results extracted from the vibrational spectra displayed in Figure 2 are also presented in Table 3. For a detailed discussion of the experimental IR spectrum, the reader is referred to ref 23.

The aforementioned difference between the **C1** and **C2** conformers on the basis of molecular interactions manifests in the vibrational spectra. For instance, the 2879 cm^{-1} mode in the IR spectrum is nicely correlated with the intense C6−H16 stretching vibration of **C1** at 2896 cm^{-1}, while it shows a discernible deviation from the 2915 cm^{-1} mode of the **C2** conformer assigned to its C7−H19 stretching vibration. Also the IR lines at 1005, 1120, 1170, and 1647 cm^{-1} and Raman modes at 1114 and 1174 cm^{-1} generally agree better with the vibrational structure of the **C1** conformer than that of **C2**. These comparisons suggest that the **C1** conformer is the major contributor to the vibrational structures observed in the experimental spectra. Therefore, we will take this view in the

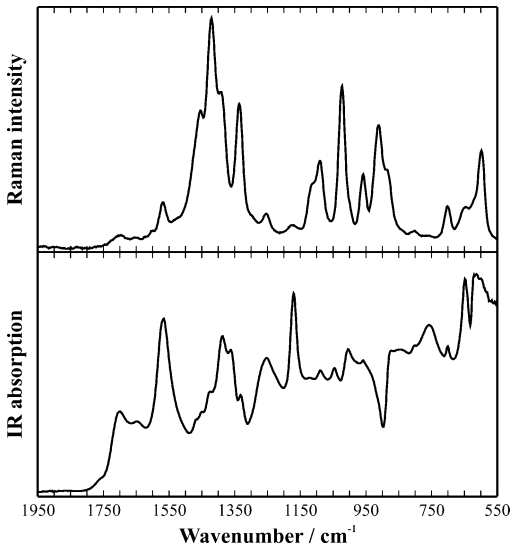

Figure 2. Experimental vibrational spectra: Raman spectrum (upper diagram) and infrared spectrum (lower diagram).

remainder of this paper when we make contact with experiments. For the sake of completeness, we also mention at the outset that in the spectral region of the CH stretching modes, small differences between the theoretically predicted frequencies and experimentally observed lines can be caused or influenced by Fermi resonances as in the case of 1,3-dialkylimidazolium bis(trifluoromethanesulfonyl)imide.[24] Specifically, since a Fermi resonance can occur when an overtone of some vibrational mode is close in frequency to the fundamental of another mode of the same symmetry, energy transfer from the latter to the former can lead to a significant change in the observable line intensities. With these caveats in mind, we consider the results in Table 3 in some detail.

One of the most salient features of our results is a downshift of the C2−H13 stretching frequency by ∼1197 cm^{-1} in the **C1** conformer with respect to the free cation value 3203 cm^{-1}. This dramatic red shift is attributed to the strong C−H···O interaction between the cation and anion, considered above. In contrast, a blue shift of ∼56 cm^{-1} is obtained for the C−H stretching of anionic CH_3 groups, which is accompanied by bond contraction in the ion pair complex. We point out that the **C2** conformer shows the same trend. Our calculations also predict that the cation−anion interactions in **C1** yield a 60 cm^{-1} red shift in the O9−C10 stretching frequency with respect to the corresponding free anion mode at 1702 cm^{-1}. The 1647 cm^{-1} mode observed in the IR spectrum is assigned to this O9−C10 local stretching mode combined with N3−C4−H14 rocking vibrations. We also notice that the interionic interactions increase the frequency separation of the doublet N−C−H rocking motions from 8 cm^{-1} (1570 and 1562 cm^{-1}) in the free cation to 30 cm^{-1} (1573 and 1543 cm^{-1}) in **C1**. Interestingly, it appears that there is only a single vibrational band present in this frequency region in the IR and Raman spectra, centered respectively at 1566 and 1569 cm^{-1}. However, a careful analysis of the comparatively broad IR structure at 1566 cm^{-1} indicates that this band is indeed constituted of an overlap of two different peaks around 1563 and 1572 cm^{-1}, consonant with the DFT results.

The contraction of the C10−C12 bond in the ion pair compared to the free anion mentioned above is accompanied by a blue shift of 54 and 48 cm^{-1} in its stretching frequency in the **C1** and **C2** conformers, respectively. Its calculated IR intensity decreases considerably in both conformers. In fact, our results in Table 3 indicate that the (asymmetric) stretching vibrations characterized by a blue shift in the complex are generally less intense than those in their free states. One exception is the N1−C7 stretch, which shows a small blue shift and intensity enhancement in the conformers compared to the isolated imidazolium ion. According to a recent study by Joseph et al.[25] on various types of hydrogen bonds, the IR intensity of red-shifted stretching vibrations tends to be higher than that of blue-shifted modes. Our results here seem to lend further support to this observation and extend it to stretching vibrations that do not involve hydrogen bonds.

Turning to ethyl and methyl groups of the cation, we notice that DFT results for their CH_2 bending vibrations are generally in good agreement with measurements. For example, the calculated frequency 1443 cm^{-1} of H16−C6−H18 rocking vibrations of **C1** compares well with the 1449 and 1454 cm^{-1} structures of the IR and Raman spectra, respectively. H19−C7−H20 twisting vibrations also show an excellent agreement between the theory and experiments in their frequency. It is interesting to notice that their IR intensity is considerably higher in the **C1** conformer than in the isolated imidazolium ion. Our calculations predict a blue shift for scissor vibrations of both H16−C6−H17 and H22−C8−H23 in the ion pair. The 1466 cm^{-1} mode observed in the IR spectrum is assigned to the latter vibrations.

In Table 3, the IR and Raman structures, respectively at 1388 and 1393 cm^{-1}, are attributed to the intense mode arising from H21−C8−H22 rocking vibrations with frequency 1392 cm^{-1} in the **C1** complex. While this assignment is very reasonable, we nevertheless point out that the IR peak at 1388 cm^{-1} could be assigned instead to the C10−C12 stretching vibrations of the acetate anion in the ion pair with the calculated frequency of 1387 cm^{-1}. Furthermore, the frequency of the corresponding mode of the free anion at 1333 cm^{-1} is very close to those of the IR and Raman spectra at 1332 and 1336 cm^{-1}, respectively. We thus do not exclude the possibility that the C10−C12 stretching vibrations are responsible for both the 1388 and 1332 cm^{-1} lines of the IR spectrum and the 1336 cm^{-1} line of the Raman spectrum. If this is indeed the case, our analysis suggests that a non-negligible population of anions in the ionic liquid phase does not participate in the strong C2−H13···O9 interactions, so that their C10−C12 stretching vibrations are close to those of free anions (see below).

The frequency of symmetric C2−N3−C4 stretching vibrations at 1008 cm^{-1} in the free cation is downshifted to 956 cm^{-1} in the **C1** conformer, in concert with the 958 cm^{-1} peak in both IR and Raman spectra. Another interesting result is that an intense vibration at 805 cm^{-1} assigned to the N1−C2−H13 wagging in the free cation essentially disappears in the **C1** conformer. The strong C2−H13···O9 interactions present in the **C1** conformer dramatically reduces the amplitude of wagging motions of H13 and thus their spectral intensity. However, both IR and Raman spectra show a weak structure at 802 cm^{-1}, which can be correlated with the 804 cm^{-1} vibration in **C2** conformer. This state of affairs suggests that a small population of **C2** is present in the ionic liquid. Another possibility is that a small number of cations do not participate in the molecular interactions in the real RTIL, analogous to the anion case mentioned above. The latter paints the picture that the RTIL is characterized by dynamic equilibrium between the energetically favored ion-pair state with strong molecular interactions ("specific solvation") and entropically favored ion states free of strong ion pair interactions ("nonspecific solvation").

TABLE 4: Electron Density in Antibonding Orbital of Different Bonds in Cation, Anion and Different Conformers of 1-Ethyl-3-methylimidazolium Acetate Ion Pair

	anion	cation	C1	C2	C3	C4
N1−C2		0.01923	0.01893	0.02118	0.01781	0.02268
C2−N3		0.01927	0.02106	0.01896	0.01568	0.01999
N3−C4		0.02120	0.02777	0.02737	0.03654	0.02774
C4−C5		0.00868	0.00882	0.00877	0.00893	0.01120
N3−C6		0.01347	0.01435	0.01493	0.01542	0.01601
N1−C7		0.03130	0.02921	0.02905	0.02845	0.03157
C7−C8		0.00857	0.01070	0.01021	0.01278	0.00792
O9−C10	0.05981		0.05871	0.05881	0.09079	0.05795
C10−O11	0.05951		0.04413	0.04411	0.02222	0.04692
C10−C12	0.11045		0.07193	0.07210	0.06701	0.07665
C2−H13		0.01057	0.13604	0.13473		0.01292
C4−H14		0.00877	0.01026	0.01028	0.01125	0.01411
C5−H15		0.00891	0.01037	0.01031	0.01134	0.01019
C6−H16		0.00255	0.03549	0.00534	0.00929	0.00321
C6−H17		0.00686	0.00759	0.00842	0.00993	0.00879
C6−H18		0.00691	0.00883	0.00930	0.01053	0.00906
C7−H19		0.01033	0.01143	0.03788	0.01245	0.01113
C7−H20		0.01241	0.01406	0.01353	0.01504	0.01508
C8−H21		0.00596	0.00653	0.00425	0.00447	0.00387
C8−H22		0.00364	0.00665	0.00699	0.00678	0.00643
C8−H23		0.00583	0.00416	0.00724	0.00728	0.01151
C12−H24	0.00594		0.00581	0.00586	0.00592	0.00302
C12−H25	0.00977		0.00609	0.00605	0.00626	0.00628
C12−H26	0.00976		0.00685	0.00686	0.00884	0.00745
[a]O9(1)	1.97704		1.96420	1.96481	1.97783	1.97169
[a]O9(2)	1.88492		1.87225	1.87283	1.85765	1.88313
[a]O10(1)	1.97703		1.96068	1.96077	1.96618	1.96267
[a]O10(2)	1.88495		1.81178	1.81255	1.79142	1.83275

[a] Lone pair electron density for oxygen atoms.

TABLE 5: Electron Density at Bond Critical Point in Cation, Anion and Different Conformers of 1-Ethyl-3-methylimidazolium Acetate Ion Pair

	anion	cation	C1	C2	C3	C4
N1−C2		0.33852	0.32909	0.33309	0.31152	0.33720
C2−N3		0.33689	0.33233	0.32858	0.31130	0.33255
N3−C4		0.30043	0.30326	0.30110	0.30241	0.29129
C4−C5		0.33393	0.33301	0.33293	0.33528	0.33644
N3−C6		0.24561	0.24621	0.25421	0.26000	0.25722
N1−C7		0.23808	0.24935	0.24161	0.25940	0.24833
C7−C8		0.24701	0.24772	0.24763	0.24747	0.24627
O9−C10	0.37543		0.35472	0.35460	0.30963	0.35716
C10−O11	0.37543		0.37927	0.37936	0.41361	0.37734
C10−C12	0.22999		0.25121	0.25115	0.25395	0.24847
C2−H13		0.29389	0.23634	0.23744	0.30272	0.29125
C4−H14		0.29161	0.28946	0.28910	0.28779	0.29125
C5−H15		0.29173	0.28916	0.28953	0.28768	0.25924
C6−H16		0.28648	0.28540	0.28310	0.28773	0.28443
C6−H17		0.28607	0.28201	0.28327	0.28167	0.28458
C6−H18		0.28607	0.28170	0.28757	0.28198	0.28474
C7−H19		0.28695	0.28889	0.28849	0.28700	0.28391
C7−H20		0.28718	0.28396	0.28274	0.28301	0.28568
C8−H21		0.27868	0.27667	0.27561	0.27824	0.27656
C8−H22		0.27899	0.27731	0.27730	0.27674	0.27713
C8−H23		0.27899	0.27893	0.27830	0.27662	0.28144
C12−H24	0.26789		0.27330	0.27346	0.27311	0.27299
C12−H25	0.27200		0.27394	0.27378	0.27538	0.27331
C12−H26	0.27198		0.27867	0.27865	0.28083	0.27772
O9----H13			0.07953	0.07884		
O11----H16			0.02524			
O11----H19				0.02436		
O9----H5						0.05937
O11----H4						0.01260
					0.05339	

Electron Density. To have a better understanding of molecular interactions in terms of electron density, we have performed a natural bond orbital (NBO) analysis using DFT (B3LYP/6-31G(d,p)). In the NBO analysis, the full density matrix is partitioned into localized one-center (e.g., core and lone pair) and two-center orbitals describing a Lewis type structure. This gives not only the total charge on each atom but also separate s- and p-electron densities. Electron delocalization is indicated by the depletion of bonding orbitals and partial occupancy of "antibonding" NBOs.

The NBO analysis clearly indicates that X−H···Y bonded interactions involving a hydrogen atom result in bond weakening, as evidenced by the increased electron density in the localized antibonding orbital. This electron density enhancement, which arises from charge transfer from the proton acceptor to proton donor, is often facilitated[16] by the lone pairs of the proton acceptors that donate electron density to the antibonding orbital of the proton donors. We found that transfer of the largest amount of electron density occurs from lone electron pairs of O9 to σ^* antibonding orbital of C2−H13 (cf. Table 4). This increase of electron density in the C2−H13 antibonding orbital leads to bond elongation in the conformers as compared to those in the free cation. According to a recent study by Hobza and co-workers,[26] there is an important difference between the red and blue-shifted vibrations; viz., the red shift results when a small portion of electron density transfers to the antibonding orbital, whereas a blue shift occurs when a larger portion of electron density transfers to the nonparticipating bonds of the proton donor. Thus by extending this, we can relate the contraction of the C10−C12 bond caused by the electron density reduction in its antibonding orbital to the blue shift of its stretching vibrations with respect to the free acetate anion. Also charge transfer from the proton acceptor (acetate anion) to the C−H antibonding orbital of the proton donor (1-ethyl-3-methylimidazolium cation) explains the weakening of the anion C−O bond and the concomitant red shift noted above.

We proceed to molecular electron density topology to gain insight into the strength of molecular interactions and related frequency shifts. The results for electron density ρ_{BCP} at bond critical points (BCPs) in the four conformers and their constituent ions are presented in Table 5. The existence of a BCP between H and O along each of the C−H···O paths identified as molecular interactions in Figure 1 and its significant electron density strongly suggest that these H···O interactions have characteristics similar to a chemical bond. In this context, the electron density ρ_{BCP} at these BCPs between H and O gauges the strength of the intermolecular hydrogen-bonded interactions,[27,28] which are manifested by distances between H and O. According to our results, the BCP of O···H along the C2−H13···O9 bond path in the **C1** conformer has the maximum electron density ($\rho_{BCP} = 0.080$ au) among all BCPs pertinent to molecular interactions of the ion pair. The corresponding BCP of **C2** is also characterized by a high ρ_{BCP} value 0.079 au. It is interesting to note that the electron density of this magnitude is much higher than the range of ρ_{BCP}, i.e., 0.002−0.035 au, proposed previously[27,28] for the X-H···Y type molecular interactions. Thus our ρ_{BCP} results confirm the highly acidic character of the hydrogen at the H13 position and provide additional support of our interpretation above that **C1** is characterized by the strongest C−H···O bonded interaction among all four conformers in Figure 1. We also notice that for the X−H···Y bonded interactions, the depletion of the electron density at the BCP of the proton donating X−H bond results in an increase in ρ_{BCP} at the BCP of the H···Y bond.

Another noteworthy feature is that changes in the ρ_{BCP} value of a bond generally correlate with its vibrational frequency shift. For instance, the imidazolium C2−H13 and acetate CO bonds, vibrational frequencies of which become red-shifted in **C1**, are

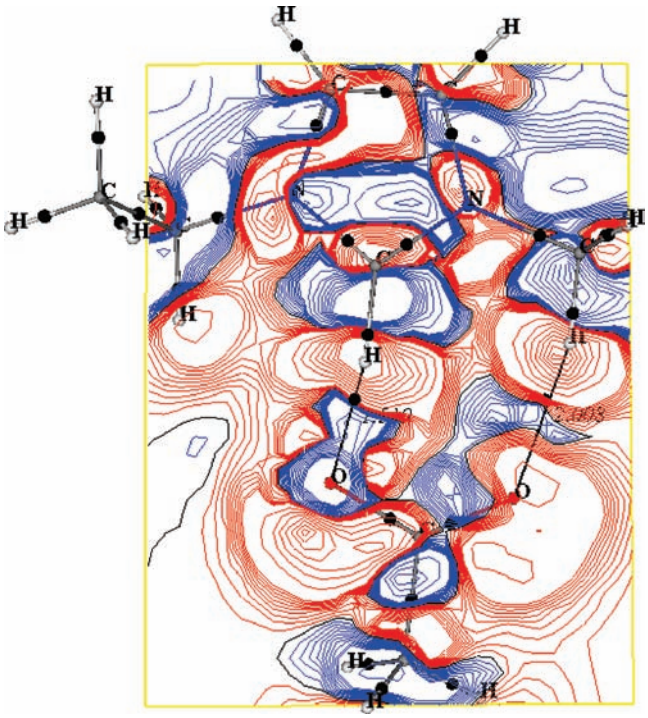

Figure 3. Difference electron density maps in the **C1** conformer. Contours in the range ±0.001 to ±0.0009 au are shown. The red and blue lines represent contours for $\Delta\rho < 0$ and $\Delta\rho > 0$, respectively. The positions of the bond critical points are marked as filled circles in black.

also characterized by reduction in their ρ_{BCP} values (cf. Table 5). On the other hand, an increase in ρ_{BCP} for acetate C10−C12 and CH_3 engenders blue shifts of their stretching vibration frequencies in **C1** relative to those in a free anion. This demonstrates that molecular electron density topology offers a useful theoretical tool to study molecular interactions and understand their influence on molecular geometry and vibrational motions.

The difference electron-density $\Delta\rho$ can be used to understand the electron density reorganization induced by hydrogen-bonded interactions. As explained above, $\Delta\rho$ is calculated by subtracting the sum of electron densities of the individual anion and cation in their free state from that of the ion pair complex. The results for $\Delta\rho$ of the **C1** conformer along a cross section of the plane bisecting the O9−C10−O11 angle are shown in the Figure 3, where the contours in the range ±0.001 to ±0.01 au are displayed. The red lines represent the contours for negative $\Delta\rho$, whereas those for $\Delta\rho > 0$ and $\Delta\rho = 0$ are shown in blue and black, respectively. We notice that the BCPs of both C−O bonds of the anion participating in the O···H interactions are situated in regions of red contours where the electron density becomes depleted upon the formation of an ion pair. This demonstrates that the red shift of the C−O stretching vibration is directly linked to its bond weakening. In contrast, the BCP of the C−C bond of the anion that shows a blue shift is located in the region where the electron density is enhanced and thus the bond is strengthened.

5. Concluding Remarks

In this article, we have studied molecular interactions in the 1-ethyl-3-methylimidazolium acetate ion pair via the NBO analysis and electron density coupled with electron density topology by employing density functional theory. Strong C−H···O interactions are manifested in the lowest energy conformers. We found that the C−C and C−H vibrations of the anion show a blue shift, while a red shift results for the cation C−H and C−O stretching vibrations. The analysis of electron density topology demonstrates that the reorganization of electron density upon the formation of the ion pair is directly related to vibrational frequency shifts. To be specific, the electron density depletion of a bond usually leads to a red shift of its vibrational frequency, whereas the density enhancement yields a blue shift. It was also found that the IR intensity generally decreases for blue-shifted stretching vibrations, while red-shifted vibrations are often accompanied by the intensity enhancement. This is congruent with a recent analysis by Joseph et al.[25]

We compared the DFT predictions of vibrational frequencies of both the most stable ion pair and free ions with measurements. Theoretically scaled frequencies of the ion pair show a good agreement with the experimental vibrational spectra obtained by infrared and Raman spectroscopy. This suggests that specific solvation via the cation−anion C2−H13···O9 interactions plays a key role in vibrational spectroscopies of the 1-ethyl-3-methylimidazolium acetate ionic liquid. Nevertheless, detailed comparison of calculations and experiments also indicates that a small amount of ions does not participate in the specific interionic C2−H13----O9 interactions in the real ionic liquid.

Our analysis here seems to indicate that the DFT approach combined with vibrational spectroscopy measurements provides a promising avenue to understand the nature of molecular interactions of ionic liquids and their consequences for, e.g., electronic structure and geometry of ions. It would thus be worthwhile in the future to attempt to improve the present theoretical description by including the nonspecific solvation effect of the surrounding ionic liquid environment on ion pairs. While the incorporation of molecular dynamics algorithms in the explicit atomic-level description of surrounding ions would be the most desirable, it would be extremely expensive computationally for ionic liquids because their high viscosity requires simulations for an extended period of time.[7] Thus the development of a continuum model description for RTILs, similar to those widely used for normal polar solvents,[29,30] would be an interesting alternative.

Acknowledgment. J.K. gratefully thanks Peter Wasserscheid and Katharina Obert for providing the ionic liquid.

Supporting Information Available: B3LYP/6-31++G(d,p) (and MP2/6-31(d,p)) results on vibrations and their comparison with B3LYP/6-31G(d,p). This material is available free of charge via the Internet at http://pubs.acs.org.

References and Notes

(1) Welton, T. *Chem. Rev.* **1999**, *99*, 2071.
(2) Wasserscheid, P.; Keim, W. *Angew. Chem., Int. Ed.* **2000**, *39*, 3772.
(3) Seddon, K. R. *J. Chem. Technol. Biotechnol.* **1997**, *68* (1), 351.
(4) Hagiwara, R.; Ito, Y. *J. Fluorine Chem.* **2000**, *105*, 221.
(5) Huddleston, J. G.; Willauer, H. W.; Swatloski, R. P.; Visser, A. E.; Rogers, R. D. *Chem. Commun.* **1998**, 1765.
(6) Broker, G. A.; Rogers, R. D. *Green Chem.* **2001**, *3*, 156.
(7) See many articles in *Acc. Chem. Res.* **2007**, *40*, Issue No. 11 and references therein.
(8) Kiefer, J.; Fries, J.; Leipertz, A. *Appl. Spectrosc.* **2007**, *61*, 1306.
(9) Lasségues, J.; Grondin, J.; Aupetit, C.; Johansson, P. J. *Phys. Chem. A* **2009**, *113*, 305. Lasségues, J.; Grondin, J.; Cavagnat, D.; Johansson, P. J. *Phys. Chem. A* **2009**, *113*, 6419. Dong, K.; Zhang, S.; Wang, D.; Yao, X. *J. Phys. Chem. A* **2006**, *110*, 9775. Talaty, E. R.; Raja, S.; Shorhaug, V. J.; Dölle, A.; Carper, W. R. *J. Phys. Chem. B* **2004**, *108*, 13177. Dhumal, N. R. *Chem. Phys.* **2007**, *342*, 245.
(10) Kiefer, J.; Obert, K.; Fries, J.; Bösmann, A.; Wasserscheid, P.; Leipertz, A. *Appl. Spectrosc.* **2009**, *63*, 1041 (and the references therein).

(11) Miloslavina, A. A.; Leipold, E.; Kijas, M.; Stark, A.; Heinemann, S. H.; Imhof, D. *J. Peptide Sci.* **2009**, *15*, 72, and the references therein.
(12) Becke, A. D. *J. Chem. Phys.* **1993**, *98*, 5684.
(13) Lee, C.; Yang, W.; Parr, R. G. *Phys. Rev.* **1988**, *B37*, 785.
(14) Frisch, M. J.; Trucks, G. W.; Schlegel, H. B.; Scuseria, G. E.; Robb, M. A.; Cheeseman, J. R.; Montgomery, J. A.; Vreven, T., Jr.; Kudin, K. N.; Burant, J. C.; Millam, J. M.; Iyengar, S. S.; Tomasi, J.; Barone, V.; Mennucci, B.; Cossi, M.; Scalmani, G.; Rega, N.; Petersson, G. A.; Nakatsuji, H.; Hada, M.; Ehara, M.; Toyota, K.; Fukuda, R.; Hasegawa, J.; Ishida, M.; Nakajima, T.; Honda, Y.; Kitao, O.; Nakai, H.; Klene, M.; Li, X.; Knox J. E.; Hratchian, H. P.; Cross, J. B.; Adamo, C.; Jaramillo, J.; Gomperts, R.; Stratmann, R. E.; Yazyev, O.; Austin, A. J.; Cammi, R.; Pomelli, C.; Ochterski, J. W.; Ayala, P. Y.; Morokuma, K.; Voth, G. A.; Salvador, P.; Dannenberg, J. J.; Zakrzewski, V. G.; Dapprich, S.; Daniels, A. D.; Strain, M. C.; Farkas, O.; Malick, D. K.; Rabuck, A. D.; Raghavachari, K.; Foresman, J. B.; Ortiz, J. V.; Cui, Q.; Baboul, A. G.; Clifford, S.; Cioslowski, J.; Stefanov, B. B.; Liu, G.; Liashenko, A.; Piskorz, P.; Komaromi, I.; Martin, R. L.; Fox, D. J.; Keith, T.; Al-Laham, M. A.; Peng, C. Y.; Nanayakkara, A.; Challacombe, M.; Gill, P. M. W.; Johnson, B.; Chen, W.; Wong, M. W. Gonzalez, C.; Pople, J. A. *Gaussion 03*; Gaussian, Inc.: Wallingford, CT, 2004.
(15) Limaye, A. C.; Gadre, S. R. *Curr. Sci. (India)* **2001**, *80*, 1298.
(16) Reed, A. E.; Curtiss, L. A.; Weinhold, F. *Chem. Rev.* **1988**, *88*, 899.
(17) Balanarayan, P.; Gadre, S. R. *J. Chem. Phys.* **2003**, *119*, 5037.
(18) Kiefer, J.; Obert, K.; Himmler, S.; Schulz, P. S.; Wasserscheid, P.; Leipertz, A. *ChemPhysChem* **2008**, *9*, 2207.
(19) Desiraju, G. R.; Steiner, T. *The Weak Hydrogen Bond in Structural Chemistry and Biology*; Oxford University Press: New York, 1999.
(20) Ennis, E.; Handy, S. T. *Curr. Org. Synth.* **2007**, *4*, 381.
(21) Koch, W.; Holthausen, M. C. *A Chemist's Guide to Density Functional Theory*; Wiley-VCH: New York, 2000. Irikura, K. K.; Johnson, R. D., III; Kacker, R. N. *J. Phys. Chem. A.* **2005**, *109*, 8430. Watson, T. M.; Hirst, J. D. *J. Phys. Chem. A.* **2002**, *106*, 7858. Dunn, M. E.; Evans, T. M.; Kirschner, K. N.; Shields, G. C. *J. Phys. Chem. A* **2006**, *110*, 303. Michalska, D.; Bienko, D. C.; Abkowicz-Bieńko, A. J.; Latajka, Z. *J. Phys. Chem.* **1996**, *100*, 17786.
(22) Bolshakov, V. I.; Rossikhin, V. V.; Voronkov, E. O.; Okovytyy, S. I.; Leszczynski, J. *J. Comput. Chem.* **2007**, *28*, 778.
(23) Kiefer, J.; Obert, K.; Bösmann, A.; Seeger, T.; Wasserscheid, P.; Leipertz, A. *ChemPhysChem* **2008**, *9*, 1317.
(24) Lassegues, J.-C.; Grondin, J.; Cavagnat, D.; Johansson, P. *J. Phys. Chem. A* **2009**, *113* (23), 6419.
(25) Joseph, J.; Jemmis, E. D. *J. Am. Chem. Soc.* **2007**, *129*, 4620.
(26) Zierkiewicz, W.; Michalska, D.; Havlas, Z.; Hobza, P. *ChemPhysChem* **2002**, *2*, 511.
(27) Kock, U.; Popelier, P. L. A. *J. Phys. Chem. A* **1995**, *99*, 9747.
(28) Popelier, P. L. A. *J. Phys. Chem. A* **1998**, *102*, 1873.
(29) Tomasi, J.; Persico, M. *Chem. Rev.* **1994**, *94*, 2027.
(30) Kim, H. J. *J. Chem. Phys.* **1996**, *105*, 6818. *J. Chem. Phys.* **1996**, *105*, 6833.

JP907394V